Effects of rock fragments on the water infiltration and hydraulic conductivity in the soils of the desert steppes of Inner Mongolia, China

Xiaolong Wu, Zhongju Meng, Xiaohong Dang, Ji Wang*

College of Desert Control Science and Engineering, Inner Mongolia Agricultural University, Hohhot, P.R. China

*Corresponding author: wangji1957@163.com

Xiaolong Wu and Zhongju Meng contributed equally to this article.

Abstract: Soils that contain rock fragments (particles > 2 mm in diameter) are distributed all over the world. The presence of these small rock fragments can have a great impact on soil water retention properties, as well as on the soil-water infiltration and vegetation restoration in semi-arid regions. To quantitatively describe the transport of water in stony soils, repacked soil cores were used to determine the infiltration rates for different rock fragment contents (0%, 10%, 20%, 30%, and 40%) and rock fragment sizes (2–5, 5–8, 8–11, and 2–11 mm). The results showed that both the content and size of the rock fragments and their interaction significantly affected the infiltration process. The infiltration rates over time and the saturated hydraulic conductivity (K_s) decreased with an increasing rock fragment content to an observed minimum value for a 40% rock fragment content. The soil-water infiltration processes were accurately described by the Kostiakov model. The measured and calculated K_s values decreased with an increasing rock fragment content, which was in accordance with the published data and in accordance with the K_s obtained by five empirical methods. The variations in the measured K_s were likely due to the variations in the soil properties caused by the soil sample repacking. The results of this study may improve the understanding of the effects of the rock fragment content and size on the infiltration processes in arid and semi-arid desert steppes.

Keywords: arid grassland; rock fragment content; rock fragment size; saturated hydraulic conductivity; soil infiltration rate

Soil-water infiltration is an important link in the land surface hydrological cycle that has significant effects on the generation of runoff, soil erosion, solute migration and water redistribution (Ebel & Moody 2013; Liu et al. 2019). Soil infiltration processes are controlled by several interacting factors, which include the soil's physical and chemical properties, the soil texture type, rock fragments in the soil, the initial soil moisture content, the land use and vegetation cover (Gonzalez-Sosa et al. 2010; Yu et al. 2015; Wang et al. 2017; Luna et al. 2018). Many soils contain large amounts of rock fragments as a result of both natural soil formation processes and human activities (Guo et al. 2010), and interest in these soils has been growing (Jomaa et al. 2012; Sohrt et al. 2014; Jiang et al. 2020). Stony soils that contain substantial amounts of rock fragments are distributed all over the world, such as in Europe (Poesen & Lavee 1994), Oceania (Pairman et al. 2011), America (Lewis et al. 2006), Asia (Ban et al. 2017a), and the Antarctic Peninsula (Golledge 2014). Rock fragments are relatively large compared to fine soil particles in the soil matrix; The content, shape, size and geological origin of the rock fragments have a

strong influence on the physical soil-water properties, especially on the soil water-retention and conductivity (Ma et al. 2010; Tetegan et al. 2012; Coppola et al. 2013). Intuitively, the presence of rock fragments reduces the cross-sectional area of the water flow, thereby reducing the hydraulic conductivity (Bouwer & Rice 1984; Childs & Flint 1990; Novák et al. 2011). However, rock fragments can create lacunar pores at the rock fragment–fine earth interface that could become paths for preferential water flow and, thus, increase the soil-water infiltration rate (Sauer & Logsdon 2002; Shi et al. 2008; Verbist et al. 2009).

The role of rock fragments in soil-water processes can be classified into two types: (1) rock fragments covering the soil surface, and (2) rock fragments embedded into the soil (Poesen & Lavee 1994). For the first type, rock fragments can reduce the slope sediment yield by depressing the sealing of the soil surface and delaying the accumulation of water, slowing the surface runoff and increasing the infiltration rate (Zavala et al. 2010; Wang et al. 2012). Rock fragments embedded into the soil constitute the second type. This type is different from the first in that rock fragments and their size, shape, content, position, and spatial distribution in the soil can strongly influence a stony soil's properties and can affect the soil-water infiltration processes (Chen et al. 2012; Al-Qinna et al. 2014) and the occurrence of runoff (Ban et al. 2017b; Gong et al. 2018). Most studies have focused on the effects of the rock fragment coverage on surface hydrological processes, whereas fewer have considered the effects of rock fragment content and size on the soil-water infiltration processes, especially for arid and semi-arid desert steppe areas.

Desert steppes are a significant type of arid and semi-arid ecosystem (Du et al. 2019). They are an extremely arid grassland type with 150–250 mm of annual precipitation (Kang et al. 2007). Soil water is one of the most important limiting factors affecting vegetation growth and the vegetation distribution pattern in arid and semi-arid areas (Wang et al. 2008; Wu et al. 2017). Under these conditions, any reduction in the soil moisture will aggravate the lack of water in both the top and deep soil layers, and even benefit the formation of dry soil layers, further endangering the sustainability of vegetation restoration (Jia et al. 2019). The rock fragments present in the surface soil are often taken as an indicator of soil erosion and soil degradation (Jiang et al. 2014; Meng et al. 2018). Currently, surface soil materials on some desert steppes contain significantly high rock fragment contents due to inappropriate land use and the negative effects of climate change (Maestre et al. 2012).

These statements define the general context in which our study takes place. The main objectives of this research were (*i*) to assess and quantify the effect of the rock fragment content and size and their interactions on the soil-water infiltration process, and (*ii*) to assess the effect of rock fragments on the saturated hydraulic conductivity of stony soils and to test the validity of the predictive models that have been proposed in the literature. The results of this study will help researchers to further understand the effects of rock fragments on the infiltration processes in arid and semi-arid areas, and will also be helpful for vegetation restoration in arid and semi-arid grasslands, which can be referred to as areas with similar natural environmental conditions.

MATERIAL AND METHODS

Study sites and soil sampling. This study was conducted at the Grassland Water Circulation and Ecological Restoration Experimental Station of the Institute of Water Resources for Pastoral Area (MWR), in Damao County (41°12'N, 111°15'E), Inner Mongolia, Northern China. This area belongs to a transition zone from a typical steppe to a desert steppe in the Inner Mongolia grassland. Based on an analysis of 20-year data, the mean annual temperature is 2.5 °C, the annual average precipitation is 281 mm, and rainfall events are unevenly distributed and occur mainly in July, August and September. We chose three sites on a hillside as sampling areas. The spacing between each site was 5 m. The soil samples were collected from a depth of 0–40 cm at each site. About 7–8 kg of soil was collected for every 5 cm layer. After the soil samples were air-dried, the samples from the same soil layer were mixed to produce one combined sample for all three sampling sites. A detailed description of the soil samples is shown in Table 1. Rock fragments were separated from the finer soil through a 2 mm sieve. All the rock fragments were approximately spherical in shape in our study. The diameter of the separated rock fragments was between 2–11 mm. The rock fragments were further sieved to obtain fractions with equivalent diameters of 2–5, 5–8, 8–11, and 2–11 mm to investigate the impact of the diameter of the rock fragments on the infiltration.

Table 1. Particle size distribution of the fine soil

Soil depth (cm)	Particle size distribution (%)			Bulk density (g/cm³)
	0.02–2 mm	0.02–0.002 mm	< 0.002 mm	
0–5	62.06 ± 2.34	28.8 ± 1.50	8.97 ± 0.86	1.32 ± 0.14
5–10	69.87 ± 3.52	23.18 ± 2.60	6.69 ± 1.00	1.44 ± 0.20
10–15	90.13 ± 0.71	7.59 ± 0.55	1.95 ± 0.20	1.62 ± 0.06
15–20	74.09 ± 2.34	19.51 ± 1.57	6.05 ± 0.73	1.58 ± 0.07
20–25	86.40 ± 3.27	10.38 ± 2.45	2.83 ± 0.70	1.62 ± 0.27
25–30	86.31 ± 1.19	10.59 ± 0.93	2.76 ± 0.29	1.61 ± 0.02
30–35	73.68 ± 1.25	20.13 ± 0.87	5.89 ± 0.38	1.51 ± 0.15
35–40	61.80 ± 2.21	29.41 ± 1.34	8.47 ± 0.83	1.50 ± 0.14

Soil column experiment. Cylindrical plexiglass tubes (50 cm tall, 15 cm inner diameter, and 0.5 cm thick) were used as the container for the experimental equipment. The soil column design was similar to the one used by Yang et al. (2004). All the separated fine soil samples (< 2 mm) were mixed well with the separated rock fragments (2–5, 5–8, 8–11, and 2–11 mm) to obtain four different weight contents (10%, 20%, 30%, and 40%), and no rock fragments (0%) as a control (CK). In order to pack the rock fragments and fine soil into the column as uniformly as possible, each layer of 5 cm was weighed separately and mixed in a container before being packed into the columns (Ma et al. 2010). The mixture of the fine soil, which had a bulk density of 1.53 g/cm³ (equal to the mean bulk density of the fine soil measured in the field), and the rock fragments were then evenly packed into an empty plexiglass column. The bottom of the column contained a plexiglass plate with evenly distributed 0.5 cm diameter holes. Before loading the soil, a coarse filter paper was placed at the bottom of the soil column to prevent the soil from flowing out from the perforated base. To avoid layering and displacement of the mixture of the fine soil and rock fragments, 5 cm per layer was continuously filled and compacted. The top of the soil column was covered with a 1 cm layer of fine gravel to reduce any disturbance from the water injection.

A Marriott device (Figure 1) was used to quickly establish and maintain a constant 5 cm water head on the soil surface for the flow experiments. The bottom boundary of the column was defined as the seepage surface, which means that once the soil at the boundary was saturated, water began to flow out. The cumulative infiltration was determined by the volume of water supplied from the Marriott bottle. During the experiments, both the cumulative

infiltration and the wetting front advance versus time were recorded with visual readings every 5 min. After the wetting front reached the bottom of the soil column, the volume of the effluent and the corresponding time were recorded every 5 min until the flow rate became constant. The total porosity was determined by weighing the soil columns before and after each experiment.

According to the dynamic process of infiltration, we took the mean infiltration rate of the first 30 min as the initial infiltration rate (IIR), and then took the
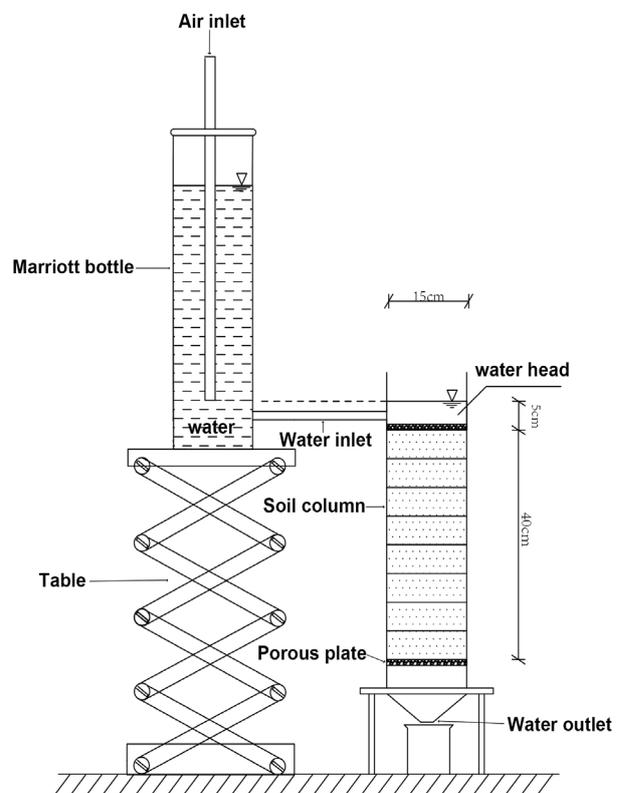

Figure 1. Experiment equipment for the water flow study

total infiltration time in which the soil infiltration reached a steady-state as the total infiltration time (TIT). The average infiltration rate during the total infiltration time was taken as average infiltration rate (AIR). The steady-state infiltration rate (SIR) is the average infiltration rate after the infiltration rate had stabilised.

Saturated hydraulic conductivity. The saturated hydraulic conductivity (K_s) of the soil columns was determined using a constant head method. A constant-head permeameter (CHP) is often used to determine the saturated conductivity of soil cores (Bagarello et al. 2006). In particular, K_s could be obtained using Darcy's law for the steady state phase of the experiment:

$$K_s = \frac{V}{tA} \times \frac{L}{H} \tag{1}$$

where:
V – the volume of the water flow (cm^3);
L – the length of the soil column (cm);
A – the cross-sectional area of the column (cm^2);
t – the time for the water flow (min);
H – the difference of the total water potentials (hydraulic heads) across the sample (cm).

To simplify the calculation of the saturated hydraulic conductivity in stony soils, multiple equations have been proposed. Based on the heat transfer theory of a non-conductive homogeneous medium, Peck and Watson (1979) derived an equation for calculating the saturated hydraulic conductivity of a stony soil with spherical (Equation (2)) and cylindrical (Equation (3)) inclusions.

$$\frac{K_{se}}{K_s} = \frac{2(1 - R_V)}{2 + R_V} \tag{2}$$

$$\frac{K_{se}}{K_s} = \frac{(1 - R_V)}{1 + R_V} \tag{3}$$

where:
K_{se}, K_s – the saturated hydraulic conductivity (cm/min) of a soil containing rock fragments and fine earth, respectively;
R_V – the volumetric rock fragment content (cm^3 per cm^3).

Ravina and Magier (1984) assumed that rock fragments are non-porous and do not change the porosity of fine soils. Hence, the relationship between the saturated hydraulic conductivity of a stony soil and a fine soil can be approximated as the volume percentage of the volume of the fine soil (Equation (4)).

$$\frac{K_{se}}{K_s} = (1 - R_V) \tag{4}$$

Similarly, Brakensiek et al. (1986) proposed a formula based on an empirical relationship, but related to the mass fraction of the rock fragments, not the volume fraction (Equation (5)).

$$\frac{K_{se}}{K_s} = (1 - R_m) \tag{5}$$

where:
R_m – the relative stone content (g/g), expressed in mass units (the mass of the stones determined by the total mass of the stony soil).

Considering the porosity of the rock fragments, Bouwer and Rice (1984) used laboratory research data on stony soils to establish the following equation:

$$\frac{K_{se}}{K_s} = \frac{e_{se}}{e_s} \tag{6}$$

where:
e_{se}, e_s – the porosities of the stony soil (total soil with rock fragments) and fine soil (total soil without rock fragments) (cm^3/cm^3), respectively.

Based on numerical simulations, Novák et al. (2011) considered that the relationship of the saturated hydraulic conductivity between a stony soil and a fine soil can be expressed using a linear equation as follows:

$$\frac{K_{se}}{K_s} = (1 - aR_V) \tag{7}$$

where:
a – an empirical parameter that considers the hydraulic resistance of the rock fragments as a function of the shape, size, and distribution. The value of the coefficient a was 1.32 in our case.

Statistical analysis. The statistical tests were conducted using the statistical software SPSS (Ver. 24.0, 2016). An analysis of variance (one-way ANOVA) was used to determine if the infiltration rates from the CK and rock fragment treatments were significantly different. A *P*-value below 0.05 is considered significant. A two-way ANOVA analysis was used to determine the influence of the rock fragment content and the size of the rock fragments and their impact on the infiltration.

RESULTS

Effects of rock fragment content and size on the cumulative infiltration and the wetting front
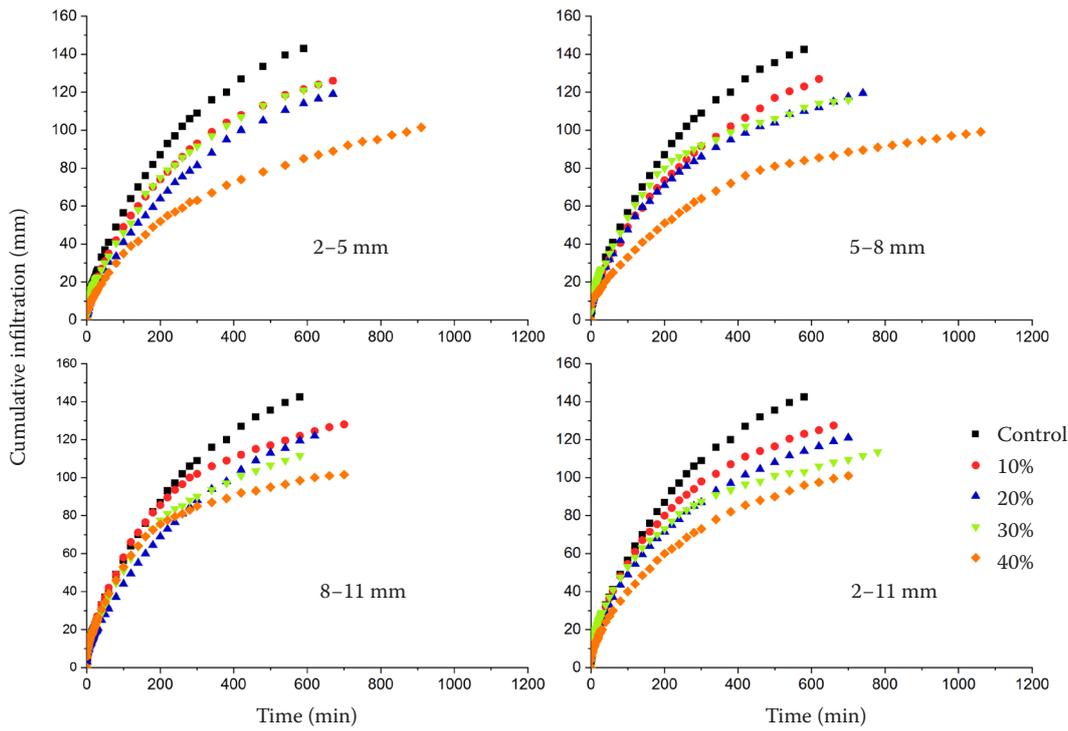
Figure 2. Relationship between the cumulative infiltration and the time

position. The time and infiltration variations of the wetting front passing through the soil column are shown in Figure 2 and 3. The cumulative infiltration decreased significantly with an increase in the rock fragment content under the same rock fragment size ($P < 0.05$). Compared with the CK, the cumulative
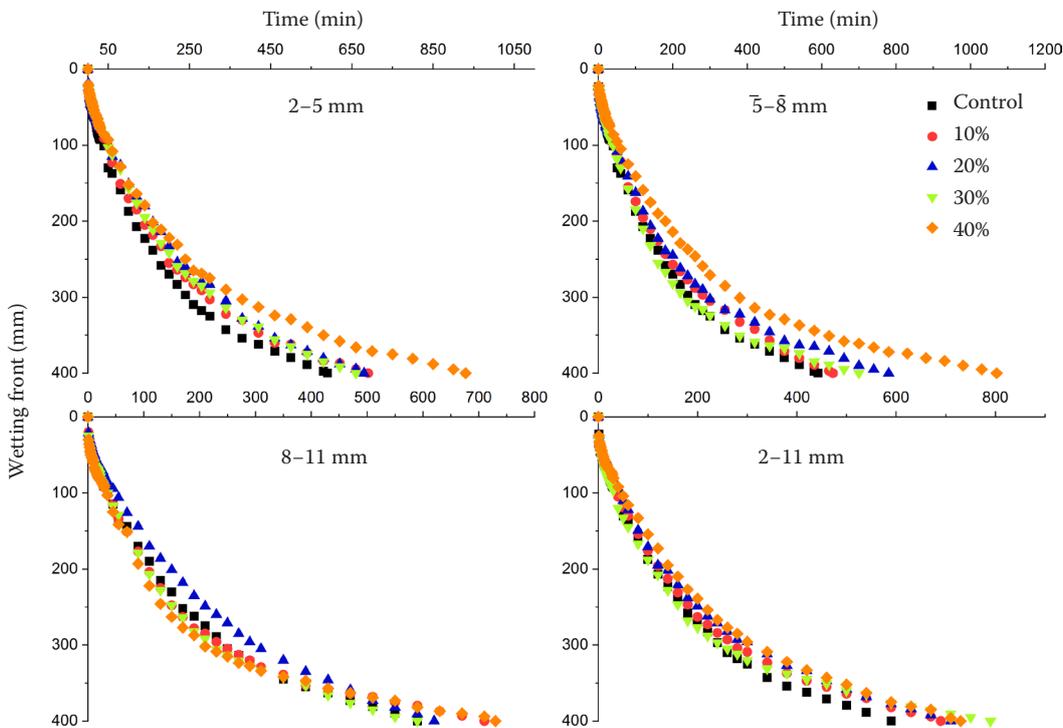

Figure 3. Relationship between the wetting front position and the time

Table 2. Infiltration time and infiltration variations of the wetting front passing through the soil column

RFC (%)	Time (min)	Accumulated infiltration (mm)	Time (min)	Accumulated infiltration (mm)	Time (min)	Accumulated infiltration (mm)	Time (min)	Accumulated infiltration (mm)
	2–5 mm		5–8 mm		8–11 mm		2–11mm	
0	590.0 ± 12.3[Aa]	143.0 ± 1.2[Aa]	590.0 ± 12.3[Aa]	143.0 ± 1.2[Aa]	590.0 ± 12.3[Aa]	143.0 ± 1.2[Aa]	590.0 ± 12.3[Aa]	143.0 ± 1.2[Aa]
10	690.0 ± 16.3[Ab]	127.8 ± 1.8[Ab]	625.0 ± 10.8[Ba]	130.3 ± 3.3[Ab]	706.7 ± 12.5[Ab]	129.3 ± 3.3[Ab]	693.3 ± 8.5[Ab]	128.3 ± 1.7[Ab]
20	681.7 ± 6.2[Ab]	120.0 ± 1.8[Ac]	781.7 ± 14.3[Bb]	120.8 ± 1.0[Ac]	616.7 ± 16.5[Ca]	122.7 ± 1.7[Ac]	711.7 ± 14.3[Ab]	121.2 ± 2.5[Ac]
30	653.3 ± 17.0[Ab]	114.3 ± 1.2[Ad]	696.7 ± 20.5[Bc]	115.7 ± 1.2[Ad]	591.7 ± 10.3[Ca]	110.2 ± 1.0[Ad]	788.3 ± 18.4[Dc]	111.8 ± 2.0[ABd]
40	930.0 ± 32.7[Ac]	102.2 ± 1.0[Ae]	1 070.0 ± 28.6[Bd]	99.3 ± 0.5[Be]	730.0 ± 20.4[Cb]	102.5 ± 1.1[Ae]	730.0 ± 16.3[Cb]	103.0 ± 0.8[Ae]

RFC – the rock fragment contents; the infiltration time is time it took for the wetting front to pass through the soil column; the capital letters indicate significant differences at $P < 0.05$ between the different rock fragment sizes at the same rock fragment content; the lowercase letters indicate significant differences at $P < 0.05$ between the different rock fragment contents at the same rock fragment size

infiltration of 2–5 mm rock fragment treatment was 10.63%, 16.08%, 20.07%%, and 28.53% lower than the CK at a 10%, 20%, 30%, and 40% rock fragment content, respectively (Table 2). However, there was no significant difference ($P > 0.05$) in the cumulative infiltration among the different rock fragment size treatments (Table 2). In addition, the presence of rock fragments significantly ($P < 0.05$) increased the

Table 3. Infiltration characteristics of the different rock fragment contents and rock fragment sizes

RFS (mm)	RFC (%)	IIR	SIR	AIR	TIT (min)
		(mm/min)			
	0	1.82 ± 0.03[a]	0.208 ± 0.006[a]	0.585 ± 0.022[a]	713.3 ± 17.0[a]
	10	1.72 ± 0.05[Ab]	0.185 ± 0.007[Ab]	0.542 ± 0.023[Aa]	790.0 ± 16.3[Ab]
2–5	20	1.20 ± 0.02[Ac]	0.162 ± 0.003[Ac]	0.466 ± 0.016[Ab]	750.0 ± 8.2[Aab]
	30	1.64 ± 0.04[Ab]	0.175 ± 0.003[Ab]	0.554 ± 0.027[Aa]	753.3 ± 12.5[Aab]
	40	1.48 ± 0.04[Ad]	0.101 ± 0.002[Ad]	0.364 ± 0.019[Ac]	1 080 ± 24.5[Ac]
	0	1.82 ± 0.03[a]	0.208 ± 0.006[a]	0.585 ± 0.022[a]	713.3 ± 17.0[a]
	10	2.23 ± 0.08[Bb]	0.189 ± 0.004[Ab]	0.688 ± 0.033[Bb]	730.0 ± 16.3[Ba]
5–8	20	2.17 ± 0.07[Bb]	0.140 ± 0.002[Bc]	0.568 ± 0.022[Ba]	933.3 ± 19.4[Bb]
	30	2.90 ± 0.08[Bc]	0.136 ± 0.005[Bc]	0.716 ± 0.024[Bb]	923.0 ± 17.7[Bb]
	40	2.39 ± 0.10[Bd]	0.081 ± 0.003[Bd]	0.415 ± 0.016[Bc]	1 302.3 ± 35.6[Bc]
	0	1.82 ± 0.03[a]	0.208 ± 0.006[a]	0.585 ± 0.022[a]	713.3 ± 17.0[a]
	10	2.12 ± 0.06[Bb]	0.158 ± 0.008[Bb]	0.853 ± 0.019[Cb]	821.3 ± 12.8[Ab]
8–11	20	1.79 ± 0.06[Ca]	0.182 ± 0.005[Cc]	0.612 ± 0.024[Ba]	693.7 ± 24.9[Ca]
	30	2.33 ± 0.08[Cc]	0.156 ± 0.005[Cb]	0.722 ± 0.025[Bc]	721.0 ± 17.6[Aa]
	40	2.38 ± 0.08[Cc]	0.123 ± 0.002[Cd]	0.576 ± 0.030[Ca]	878.3 ± 27.4[Cc]
	0	1.82 ± 0.03[a]	0.208 ± 0.006[a]	0.585 ± 0.022[a]	713.3 ± 17.0[a]
	10	2.53 ± 0.09[Cb]	0.182 ± 0.004[Ab]	0.735 ± 0.028[Bb]	746.7 ± 12.5[Ba]
2–11	20	2.66 ± 0.10[Dbc]	0.155 ± 0.003[Ac]	0.688 ± 0.020[Cbc]	825.7 ± 17.8[Db]
	30	2.75 ± 0.10[Bc]	0.129 ± 0.003[Bd]	0.654 ± 0.023[Bc]	909.0 ± 23.7[Bc]
	40	1.76 ± 0.06[Ba]	0.122 ± 0.004[Cd]	0.499 ± 0.018[Dd]	867.7 ± 19.3[Cd]

RFS – the rock fragment sizes; RFC – the rock fragment contents; IIR – the initial infiltration rate; SIR – the steady-state infiltration rate; AIR – the average infiltration rate; TIT – the total infiltration time; the capital letters indicate significant differences at $P < 0.05$ between the different rock fragment sizes at the same rock fragment content; the lowercase letters indicate significant differences at $P < 0.05$ between the different rock fragment contents at the same rock fragment size

infiltration time for all the treatments (Figures 2, 3). For the CK treatment, the times required for the wetting fronts to reach the 400 mm position were significantly ($P < 0.05$) lower than in the rock fragment treatments (Table 2). At the end of the experiment, all of the wetting fronts reached the 400 mm position at different times. The time required for the wetting front to reach the 400 mm position first increased and then decreased with an increasing rock fragment size. For the 2–5 and 5–8 mm rock fragments, the time required for the wetting front to reach the 200 and 400 mm positions was the shortest. Inversely, for the 8–11 mm rock fragment size, the time required for the wetting front to reach the 200 and 400 mm positions was at first the longest, then became the shortest.

Effects of rock fragments on the infiltration rate. The soil infiltration rate is the volume flux of the water flowing into the profile per unit of soil surface area; it is also an important indicator to characterise the soil infiltration performance. The infiltration rate rapidly decreased during the initial state and then gradually stabilised in our study. The infiltration characteristics from the different treatments are shown in Table 3. The SIR (steady-state infiltration rate) decreased significantly with an increase in the rock fragment content under the same rock fragment size ($P < 0.05$). Similarly, the TIT (total infiltration time) significantly increased with an increase in the rock fragment content. The lowest SIR values were found at a 40% rock fragment content among the different treatments. For the 2–5 mm rock fragment treatment, the CK exhibited higher infiltration rates than the rock fragment treatment and the IIR (initial infiltration rate) and the AIR (average infiltration rate) were significantly ($P < 0.05$) decreased with an increase in the rock fragment content (Table 3). However, the IIR and AIR of the CK were significantly ($P < 0.05$) lower than for the 5–8, 8–11, and 2–11 mm rock fragment treatments.

The two-way ANOVA analyses showed that the rock fragment content, rock fragment size and the interaction effect of the rock fragment content and size significantly ($P < 0.01$) affected the SIR, IIR, AIR, and TIT. In particular, the two-way ANOVA showed that the rock fragment content significantly ($P < 0.01$) affected the TP (total porosity), but there was not a significant ($P > 0.05$) effect on the TP due to the rock fragment size (Table 4).

Infiltration models. We fitted the experimental data with Kostiakov's (1932) and Philip's (1969) infiltration models (Equations (8) and (9), respectively) to further analyse the soil infiltration rate data and the applicability of the infiltration models in semi-arid stony soils. The fitting parameters are shown in Table 5.

$$f(t) = at^{-b} \tag{8}$$

$$f(t) = 0.5St^{1/2} + A \tag{9}$$

where:
$f(t)$ – the infiltration rate (mm/min);
t – the time (min);
a, b – are Kostiakov model infiltration parameters;
S – the soil sorptivity (mm/min);
A – the stable infiltration rate (mm/min).

Table 5 shows that the relationship between the infiltration rate and time were well fitted with the traditional infiltration models, the determination coefficient (R^2) for Philip's model ranged from 0.903 to 0.995, and that for Kostiakov's model was 0.957 to 0.999. Obviously, the determination coefficient (R^2) of the Kostiakov model was higher. The root mean square error (RMSE) is the part of the total variation that cannot be explained by regression covariates. As the root mean square error (RMSE) approaches 0, it indicates that the selected model has a better fit. The root mean square error (RMSE) of Philip's model was (0.039–0.261 mm/min) higher than that of

Table 4. Two-way ANOVA of the rock contents and rock size for the infiltration process

Variable	IIR	SIR	AIR	TIT (min)	TP (cm³/cm³)
		(mm/min)			
A	391.197**	23.632**	97.455**	110.601**	0.174ns
B	126.046**	502.282**	127.662**	304.423**	406.253**
A × B	72.147**	22.221**	13.513**	57.09**	2.695*

A – the rock fragment size; B – the rock fragment content; A × B is the interaction of A and B; IIR – the initial infiltration rate; SIR – the steady-state infiltration rate; AIR – the average infiltration rate; TIT – the total infiltration time; TP – the total porosity; *,**significant correlations at $P < 0.05$, 0.01, respectively; nsdenotes significant correlations at $P > 0.05$

Kostiakov's model (0.034–0.120 mm/min) (Table 5). However, the *A* values in Philip's Equation were found to be mostly negative in our study, which was not consistent with the physical meaning of Philip's Equation. Hence, Kostiakov's model could better fit the relationship between the soil infiltration rate and the time in our study.

Effects of rock fragments on the saturated hydraulic conductivity. Figure 4 shows the observed functional relationship between the saturated hydraulic conductivity (K_s) of the different rock fragment contents and the size experimental treatments, and the model comparison with the predicted values of Equations (2), (4), (5), (6), and (7). It can be seen from Figure 4 that the observed saturated hydraulic conductivity did not increase or decrease uniformly with an increase in the rock fragment content, but showed a fluctuating decreasing trend. The saturated

hydraulic conductivity of CK was always higher than that of the rock fragment treatments (Figure 4). For the 2–5 mm rock fragment treatment, the saturated hydraulic conductivities of the different rock fragment contents were CK (0.019 mm/min), 10% content (0.017 mm/min), 30% content (0.016 mm/min), 20% content (0.015 mm/min), and 40% content (0.008 mm/min). With an increase in the rock fragment content, the saturated hydraulic conductivity of the different rock fragment treatments showed an overall downward trend. When the rock fragment content was 40%, the value of the saturated hydraulic conductivity was the smallest in all the experimental treatments.

As shown in Figure 4, for the 5–8 mm rock fragment treatment, the K_s values calculated by the Ravina-Magier (1984), Bouwer-Rice (1984), Brakensiek et al. (1986), Novák et al. (2011), and Peck-Watson (1979)
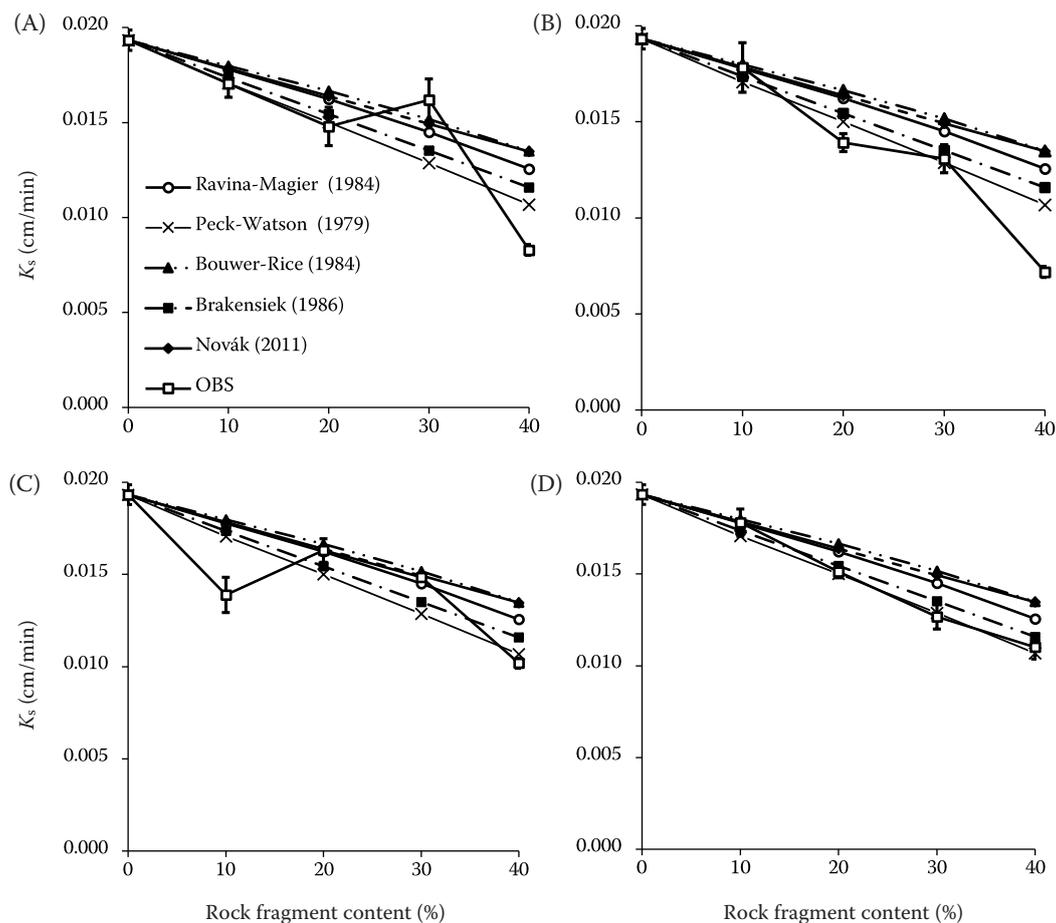

Figure 4. Influence of the rock fragment size 2–5 mm (A), 5–8 mm (B), 8–11 mm (C), 2–11 mm (D) and the rock fragment content on the saturated hydraulic conductivity (K_s), and the comparison of the prediction models for the saturated hydraulic conductivity of the stony soil
The error bar is the standard error of the measured value

Table 5. Infiltration model and parameters under the different rock fragment sizes and content

Size (mm)	RFC (%)	Philip's equation fitting results				Kostiakov's equation fitting results			
		S	A	R^2	RMSE	a	b	R^2	RMSE
	0	7.194	0.159	0.948	0.122	3.327	0.384	0.982	0.073
	10	7.482	0.074	0.992	0.049	3.681	0.455	0.991	0.053
2–5	20	4.630	0.152	0.934	0.091	2.137	0.354	0.983	0.047
	30	6.725	0.118	0.974	0.082	3.161	0.407	0.992	0.045
	40	7.322	−0.042	0.924	0.145	4.337	0.631	0.957	0.109
	10	11.334	−0.083	0.957	0.178	6.411	0.607	0.981	0.118
	20	10.020	−0.039	0.985	0.086	5.231	0.541	0.989	0.075
5–8	30	13.850	−0.127	0.979	0.144	7.476	0.585	0.989	0.103
	40	12.132	−0.192	0.903	0.261	7.947	0.763	0.990	0.084
	10	8.779	0.091	0.930	0.176	4.102	0.426	0.948	0.153
	20	7.610	0.056	0.955	0.123	3.708	0.459	0.957	0.120
8–11	30	11.420	−0.100	0.959	0.175	6.446	0.612	0.984	0.110
	40	11.248	−0.081	0.991	0.077	5.934	0.561	0.997	0.045
	10	12.147	−0.086	0.978	0.137	6.589	0.578	0.990	0.090
	20	12.551	−0.119	0.984	0.116	6.723	0.581	0.994	0.070
2–11	30	13.053	−0.123	0.992	0.085	6.927	0.575	0.999	0.034
	40	8.002	−0.011	0.995	0.039	4.082	0.517	0.996	0.036

RFC – the rock fragment contents; R^2 – the coefficient of determination for the fit of the Philip's and Kostiakov's equations; RMSE – the root mean square error

Equations were all overestimated, and for the 2–5, 8–11, and 2–11 mm rock fragment treatments, the saturated hydraulic conductivity values calculated by the Peck-Watson Equation were the greatest and the closest to the observed saturated hydraulic conductivity values.

DISCUSSION

Effects of the rock fragment content and size on the soil water infiltration process. The soil-water infiltration is a very complex process in the hydrologic cycle. Rock fragments have a significant influence on the soil hydrological processes through their content, size, shape, orientation, and degree of weathering (Brouwer & Anderson 2000; Cousin et al. 2003; Zhang et al. 2016). In our study, as shown in Figures 2 and 3, the cumulative infiltration and position of the wetting front mainly depended on the rock fragment content, while the size of rock fragments was secondary, and the SIR decreased significantly with an increase in the rock fragment content under the same rock fragment size. The reduction in the soil infiltration rate may have been caused by the decreasing soil total porosity which

was significantly related to the rock fragment content (Table 4). This indicated that the rock fragments increased the resistance within the soils compared with the fine soil fractions, and that the size of this reduction largely depended on the content of the rock fragments, which was consistent with the results of Ma et al. (2010) and Ilek et al. (2019). Consistent with the findings of Zhou et al. (2009), we also obtained minimum infiltration values under the 40% rock fragment content in our study. In Yang et al. (2013) and Mao et al. (2011), however, the lowest infiltrations were reported under the 50% fraction and the 20–30% fraction, respectively. The presence of stones can affect the soil-water infiltration process in several ways. The rock fragments reduce the effective cross-sectional area for infiltrating and redistributing the water. Hence, an increase in the rock fragment content in the soil causes the tortuosity of the flow to increase (Childs & Flint 1990; Sauer & Logsdon 2002; Hlaváčiková et al. 2016). In contrast, the infiltration may be increased since the space between the rock fragments is not completely filled with fine phases or because the contraction-expansion phenomenon may produce temporary lacunar pores which can cause preferential flow and

improve the soil infiltration performance (Shi et al. 2008; Verbist et al. 2009; Zhou et al. 2011; Nasri et al. 2015). Our results indicated that the infiltration rate of the soils with the rock fragments does not always decrease with an increase in the rock fragment content. This effect was more obvious when the content of the rock fragments was about 30%. This could be due to the lacunar pores (pores on the interface between the rock fragments and the fine soil) and the changes in the pore structure of the fine soil, which may have a greater positive impact than the negative impact of the gravel to reduce the water cross section and increase the pore curvature; Zhou et al. (2009), Ma et al. (2010), and Ilek et al. (2019) also produced similar results.

The mean size of the rock fragments affects the soil-water infiltration process as well. Rock fragments of different sizes often lead to different levels of continuity, and the size of the rock fragments can explain the difference in the water flow around the rock fragments (Zhang et al. 2016). In our study, we observed that the resistance of the 2–5 and 5–8 mm rock fragments to the water flow at a 40% content was greater than that of the 8–11 and 2–11 mm rock fragment sizes (Figure 2), and in the initial infiltration stage, the 5–8, 8–11, and 2–11 mm gravel showed a higher infiltration rate than that of the CK. This result was consistent with previous studies (Danalatos et al. 1995; Katra et al. 2008; Beckers et al. 2016). This could be due to the specific surface area of the large-size rock fragments being larger than that of the small-size rock fragments, and the fact that the large-size rock fragments have more fine soil around them than the small-size rock fragments, so their matrix suction is greater and the initial infiltration rate is larger.

Effects of the rock fragment content and size on the hydraulic conductivity of the saturated soils. Due to the large spatial variability in the rock fragment distribution, determining the soil hydraulic characteristics is complex and difficult (Sauer & Logsdon 2002, Tetegan et al. 2012). The results of the present study confirmed that the rock fragments significantly decreased the soil saturated hydraulic conductivity compared with the CK, and the K_s decreased proportionally with an increasing rock fragment content (Figure 4). This reduction in the K_s may have been caused by the decreasing soil total porosity, which was positively correlated to the rock fragment content (Table 4). This result was consistent with previous studies (Ma et al. 2010; Hlaváčiková &

Novák 2014; Gargiulo et al. 2016). We observed that the effect of the rock fragment size on the saturated hydraulic conductivity was not obvious in our study (Figure 4). However, previous studies indicated that large rock fragment sizes decreased the relative effective saturated hydraulic conductivity more than smaller rock fragments with the same total volume (Ma & Shao 2008; Novák et al. 2011). This could be due to fact that the sizes of the rock fragments studied by Ma and Shao (2008) and Novák et al. (2011) were 5–40 and 50–200 mm, respectively, which was much larger than the 2–11 mm size in our study. In addition, the total porosity was considered to be an important factor affecting the saturated hydraulic conductivity. However, the rock fragment size had no significant effect on the total porosity in our study (Table 4), indicating that the rock fragment size may have little effect on the K_s. A reduction in the soil porosity with an increased rock fragment content is one of the most important factors affecting the K_s of stony soils, but other factors may also have an effect, such as the rock fragment shape and orientation. Taking ellipsoid rock fragments as an example, the effect on the K_s is different if this type of rock fragment is oriented horizontally or vertically.

Furthermore, by comparing the saturated hydraulic conductivity predicted by the five methods, it was found that the predicted values of all five methods were overestimated for the 5–8 mm rock fragment treatment. Similarly, for the 2–5, 8–11, and 2–11 mm rock fragment treatment, the K_s values predicted by Equations (4), (5), (6), and (7) were higher than the measured saturated hydraulic conductivity, and the predicted values of Equation (6) deviated the most from the measured values. Although the results predicted by Equation (2) could not reflect the microscopic changing trend of the saturated hydraulic conductivity of the stony soils with the rock fragment content, they could roughly reflect the true magnitude of the hydraulic conductivity of the saturated soils in our study. The Peck-Watson (1979) method treats rock fragments as an impermeable medium, and it partially considers the effect of rock fragment permeability on the soil hydraulic properties. However, the Bouwer-Rice (1984) method considers the water permeability of a fine soil and rock fragments, which is very important for stony soils with high porosity due to the rock fragments (Ma et al. 2010). The permeability of the rock fragments in our study was extremely low; therefore, the water flow channel and effective porosity were the main influencing factors.

Zhou et al. (2009) similarly reported that as the rock fragment content increases, both Equation (2) and (5) overestimate the K_s value, especially in terms of the lower rock fragment content. These findings indicated that the above prediction models are not appropriate for all situations, particularly for stony soils containing smaller rock fragments. Therefore, further investigation is required to determine the hydraulic properties of stony soils and develop new models or adjust the existing ones. The trends in the saturated hydraulic conductivity were consistent with the trends in the cumulative infiltration.

CONCLUSIONS

This study demonstrated that both the content and size of the rock fragments in stony soils and their interaction had significant effects on the soil-water infiltration process. The saturated hydraulic conductivity of the stony soils decreased with an increasing rock fragment content to an observed minimum when the rock fragment content was at the highest proportion used in this study (40%). Soils with different sizes of rock fragments, but with the same rock fragment content, led to similar values of K_s. in other words, the rock fragment size had only a minor influence on K_s.

Our results indicated that the Kostiakov infiltration equation can better fit the infiltration curves of the studied stony soils than the Philip model, with a Kostiakov coefficient of determination R^2 and root mean square error (RMSE) value of 0.983 and 0.080, respectively. The variation in the porosity with an increased rock fragment content is one of the most important factors affecting the hydraulic properties of stony soils, but other factors may also have an effect. In this paper, only disturbed soils were considered; the analysis of undisturbed soils could lead to different results. The rock fragment shape and orientation, which were not considered in this paper, as well as repacking the fine earth with different lacunar pores, could lead to more realistic results.

The results of these experiments showed that K_s decreased proportionally with an increasing rock fragment content. This was in accordance with the K_s values obtained by the five empirical methods used. The differences may have been due to the variation in the soil properties during the soil sample repacking. The K_s values predicted by Equations (4), (5), (6), and (7) were overestimated; the Peck-Watson equation was the best approximation of the measured data.

All the methods of the K_s calculation used in this study were empirical ones and took the rock fragment content into account only. The porosity was linked to the rock fragment content in this study. Systematic research is required to better understand the water transport in stony soils.

REFERENCES

Al-Qinna M., Scott H.D., Brye K.R., Van Brahana J., Sauer T.J., Sharpley A. (2014): Coarse fragments affect soil properties in a mantled-karst landscape of the Ozark Highlands. Soil Science, 179: 42–50.

Bagarello V., Elrick D.E., Iovino M., Sgroi A. (2006): A laboratory analysis of falling head infiltration procedures for estimating the hydraulic conductivity of soils. Geoderma, 135: 322–334.

Ban Y., Lei T., Feng R., Qian D. (2017a): Effect of stone content on water flow velocity over Loess slope: Frozen soil. Journal of Hydrology, 554: 792–799.

Ban Y., Lei T., Gao Y., Qu L. (2017b): Effect of stone content on water flow velocity over Loess slope: non-frozen soil. Journal of Hydrology, 549: 525–533.

Beckers E., Pichault M., Pansak W., Degré A., Garré S. (2016): Characterization of stony soils' hydraulic conductivity using laboratory and numerical experiments. Soil, 2: 421–431.

Bouwer H., Rice R. (1984): Hydraulic properties of stony vadose zones. Ground Water, 22: 696–705.

Brakensiek D., Rawls W., Stephenson G. (1986): Determining the saturated hydraulic conductivity of a soil containing rock fragments. Soil Science Society of America Journal, 50: 834–835.

Brouwer J., Anderson H. (2000): Water holding capacity of ironstone gravel in a typic plinthoxeralf in southeast Australia. Soil Science Society of America Journal, 64: 1603–1608.

Chen H., Liu J., Zhang W., Wang K. (2012): Soil hydraulic properties on the steep karst hillslopes in northwest Guangxi, China. Environmental Earth Sciences, 66: 371–379.

Childs S.W., Flint A.L. (1990): Physical properties of forest soils containing rock fragments. In: Gessel S.P., Lacate D.S., Weetman G.F., Power R.F. (eds): Sustained Productivity of Forest Soils. Proc. 7th North American Forest Soils Conf., Vancouver, July 24–28, 1988: 95–121.

Coppola A., Dragonetti G., Comegna A., Lamaddalena N., Caushi B., Haikal M., Basile A.J.S., Research T. (2013): Measuring and modeling water content in stony soils. Soil and Tillage Research, 128: 9–22.

Cousin I., Nicoullaud B., Coutadeur C. (2003): Influence of rock fragments on the water retention and water percolation in a calcareous soil. Catena, 53: 97–114.

Danalatos N., Kosmas C., Moustakas N., Yassoglou N. (1995): Rock fragments II. Their impact on soil physical properties and biomass production under Mediterranean conditions. Soil Use and Management, 11: 121–126.

Du H., Zuo X., Li S., Wang T., Xue X. (2019): Wind erosion changes induced by different grazing intensities in the desert steppe, Northern China. Agriculture, Ecosystems & Environment, 274: 1–13.

Ebel B.A., Moody J.A. (2013): Rethinking infiltration in wildfire-affected soils. Hydrological Processes, 27: 1510–1514.

Gargiulo L., Mele G., Terribile F. (2016): Effect of rock fragments on soil porosity: a laboratory experiment with two physically degraded soils. European Journal of Soil Science, 67: 597–604.

Golledge N.R. (2014): Selective erosion beneath the Antarctic Peninsula Ice Sheet during LGM retreat. Antarctic Science, 26: 698–707.

Gong T., Zhu Y., Shao M.A. (2018): Effect of embedded-rock fragments on slope soil erosion during rainfall events under simulated laboratory conditions. Journal of Hydrology, 563: 811–817.

Gonzalez-Sosa E., Braud I., Dehotin J., Lassabatère L., Angulo-Jaramillo R., Lagouy M., Branger F., Jacqueminet C., Kermadi S., Michel K. (2010): Impact of land use on the hydraulic properties of the topsoil in a small French catchment. Hydrological Processes, 24: 2382–2399.

Guo T., Wang Q., Li D., Zhuang J. (2010): Effect of surface stone cover on sediment and solute transport on the slope of fallow land in the semi-arid loess region of northwestern China. Journal of Soils and Sediments, 10: 1200–1208.

Hlaváčiková H., Novák V. (2014): A relatively simple scaling method for describing the unsaturated hydraulic functions of stony soils. Journal of Plant Nutrition and Soil Science, 177: 560–565.

Hlaváčiková H., Novák V., Šimůnek J. (2016): The effects of rock fragment shapes and positions on modeled hydraulic conductivities of stony soils. Geoderma, 281: 39–48.

Ilek A., Kucza J., Witek W. (2019): Using undisturbed soil samples to study how rock fragments and soil macropores affect the hydraulic conductivity of forest stony soils: Some methodological aspects. Journal of Hydrology, 570: 132–140.

Jia X., Shao M., Yu D., Zhang Y., Binley A. (2019): Spatial variations in soil-water carrying capacity of three typical revegetation species on the Loess Plateau, China. Agriculture, Ecosystems & Environment, 273: 25–35.

Jiang Z., Lian Y., Qin X. (2014): Rocky desertification in Southwest China: impacts, causes, and restoration. Earth-Science Reviews, 132: 1–12.

Jiang Z.-D., Wang Q.-B., Adhikari K., Brye K.R., Sun Z.-X., Sun F.-J., Owens P.R. (2020): A vertical profile imaging method for quantifying rock fragments in gravelly soil. Catena, 193: 104590.

Jomaa S., Barry D.A., Brovelli A., Heng B., Sander G.C., Parlange J.-Y., Rose C.W. (2012): Rain splash soil erosion estimation in the presence of rock fragments. Catena, 92: 38–48.

Kang L., Han X., Zhang Z., Sun O.J. (2007): Grassland ecosystems in China: review of current knowledge and research advancement. Philosophical Transactions of the Royal Society B: Biological Sciences, 362: 997–1008.

Katra I., Lavee H., Sarah P. (2008): The effect of rock fragment size and position on topsoil moisture on arid and semi-arid hillslopes. Catena, 72: 49–55.

Kostiakov A.N. (1932): On the dynamics of the coefficient of water percolation in soils and the necessity of studying it from the dynamic point of view for the purposes of amelioration. Transactions of the 6th Committee International Society of Soil Science, Russia, Part A: 17–21.

Lewis S.A., Wu J.Q., Robichaud P.R. (2006): Assessing burn severity and comparing soil water repellency, Hayman Fire, Colorado. Hydrological Processes, 20: 1–16.

Liu Y., Cui Z., Huang Z., López-Vicente M., Wu G.-L. (2019): Influence of soil moisture and plant roots on the soil infiltration capacity at different stages in arid grasslands of China. Catena, 182: 104147.

Luna L., Vignozzi N., Miralles I., Solé-Benet A. (2018): Organic amendments and mulches modify soil porosity and infiltration in semiarid mine soils. Land Degradation & Development, 29: 1019–1030.

Ma D., Shao M. (2008): Simulating infiltration into stony soils with a dual-porosity model. European Journal of Soil Science, 59: 950–959.

Ma D., Shao M., Zhang J., Wang Q. (2010): Validation of an analytical method for determining soil hydraulic properties of stony soils using experimental data. Geoderma, 159: 262–269.

Maestre F.T., Salguero-Gomez R., Quero J.L. (2012): It is getting hotter in here: determining and projecting the impacts of global environmental change on drylands. Philosophical Transcactions of the Royal Society of London, Series B, Biological Sciences, 367: 3062–3075.

Mao T., Zhu Y., Shao M., Wu B. (2011): Characteristics of runoff and infiltration in stony soils under simulated rainfall conditions. Chinese Journal of Soil Science, 42: 1214–1218. (in Chinese)

Meng Z., Dang X., Gao Y., Ren X., Ding Y., Wang M. (2018): Interactive effects of wind speed, vegetation coverage and soil moisture in controlling wind erosion in a temperate desert steppe, Inner Mongolia of China. Journal of Arid Land, 10: 534–547.

Nasri B., Fouché O., Torri D. (2015): Coupling published pedotransfer functions for the estimation of bulk den-

sity and saturated hydraulic conductivity in stony soils. Catena, 131: 99–108.

Novák V., Kňava K., Šimůnek J. (2011): Determining the influence of stones on hydraulic conductivity of saturated soils using numerical method. Geoderma, 161: 177–181.

Pairman D., Belliss S.E., Cuff J., McNeill S.J. (2011): Detection and mapping of irrigated farmland in Canterbury, New Zealand. In: IEEE International Geoscience and Remote Sensing Symposium, Vancouver, July 24–29, 2011: 696–699.

Peck A., Watson J.D. (1979): Hydraulic conductivity and flow in non-uniform soil. In: Workshop on Soil Physics and Field Heterogeneity, Canberra, Feb 12–14, 1979: 31–39.

Philip J.R. (1969): Theory of infiltration. Advances in Hydroscience, 5: 215–296.

Poesen J., Lavee H. (1994): Rock fragments in top soils: significance and processes. Catena, 23: 1–28.

Ravina I., Magier J. (1984): Hydraulic conductivity and water retention of clay soils containing coarse fragments. Soil Science Society of America Journal, 48: 736–740.

Sauer T.J., Logsdon S.D. (2002): Hydraulic and physical properties of stony soils in a small watershed. Soil Science Society of America Journal, 66: 1947–1956.

Shi Z., Wang Y., Yu P., Xu L., Xiong W., Guo H. (2008): Effect of rock fragments on the percolation and evaporation of forest soil in Liupan Mountains, China. Acta Ecologica Sinica, 28: 6090–6098. (in Chinese)

Sohrt J., Ries F., Sauter M., Lange J. (2014): Significance of preferential flow at the rock soil interface in a semi-arid karst environment. Catena, 123: 1–10.

Tetegan M., Pasquier C., Besson A., Nicoullaud B., Bouthier A., Bourennane H., Desbourdes C., King D., Cousin I. (2012): Field-scale estimation of the volume percentage of rock fragments in stony soils by electrical resistivity. Catena, 92: 67–74.

Verbist K., Baetens J., Cornelis W., Gabriels D., Torres C., Soto G. (2009): Hydraulic conductivity as influenced by stoniness in degraded drylands of Chile. Soil Science Society of America Journal, 73: 471–484.

Wang H., Zhang G.-H., Liu F., Geng R., Wang L.-J. (2017): Temporal variations in infiltration properties of biological crusts covered soils on the Loess Plateau of China. Catena, 159: 115–125.

Wang X.-P., Cui Y., Pan Y.-X., Li X.-R., Yu Z., Young M. (2008): Effects of rainfall characteristics on infiltration and redistribution patterns in revegetation-stabilized desert ecosystems. Journal of Hydrology, 358: 134–143.

Wang X., Li Z., Cai C., Shi Z., Xu Q., Fu Z., Guo Z. (2012): Effects of rock fragment cover on hydrological response and soil loss from Regosols in a semi-humid environment in South-West China. Geomorphology, 151: 234–242.

Wu G.-L., Liu Y., Yang Z., Cui Z., Deng L., Chang X.-F., Shi Z.-H. (2017): Root channels to indicate the increase in soil matrix water infiltration capacity of arid reclaimed mine soils. Journal of Hydrology, 546: 133–139.

Yang H., Rahardjo H., Wibawa B., Leong E.-C. (2004): A soil column apparatus for laboratory infiltration study. Geotechnical Testing Journal, 27: 347–355.

Yang Y.-F., Wang Q.-J., Zhuang J. (2013): Estimating hydraulic parameters of stony soils on the basis of one-dimensional water absorption properties. Acta Agriculturae Scandinavica, Section B – Soil & Plant Science, 63: 304–313.

Yu M., Zhang L., Xu X., Feger K.H., Wang Y., Liu W., Schwärzel K. (2015): Impact of land-use changes on soil hydraulic properties of Calcaric Regosols on the Loess Plateau, NW China. Journal of Plant Nutrition and Soil Science, 178: 486–498.

Zavala L.M., Jordán A., Bellinfante N., Gil J. (2010): Relationships between rock fragment cover and soil hydrological response in a Mediterranean environment. Soil Science and Plant Nutrition, 56: 95–104.

Zhang Y., Zhang M., Niu J., Li H., Xiao R., Zheng H., Bech J. (2016): Rock fragments and soil hydrological processes: significance and progress. Catena, 147: 153–166.

Zhou B.B., Shao M.A., Shao H.B. (2009): Effects of rock fragments on water movement and solute transport in a Loess Plateau soil. Comptes Rendus Geoscience, 341: 462–472.

Zhou B.B., Shao M.A., Wang Q.J., Yang T. (2011): Effects of different rock fragment contents and sizes on solute transport in soil columns. Vadose Zone Journal, 10: 386–393.